TISSUE ENGINEERING: Part A
Volume 20, Numbers 23 and 24, 2014

DOI: 10.1089/ten.tea.2013.0659

Alginate Encapsulation of Human Embryonic Stem Cells to Enhance Directed Differentiation to Pancreatic Islet-Like Cells

Thomas Richardson, BS,[1] Prashant N. Kumta, PhD,[1,2] and Ipsita Banerjee, PhD[1]

The pluripotent property of human embryonic stem cells (hESCs) makes them attractive for treatment of degenerative diseases such as diabetes. We have developed a stage-wise directed differentiation protocol to produce alginate-encapsulated islet-like cells derived from hESCs, which can be directly implanted for diabetes therapy. The advantage of alginate encapsulation lies in its capability to immunoisolate, along with the added possibility of scalable culture. We have evaluated the possibility of encapsulating hESCs at different stages of differentiation. Encapsulation of predifferentiated cells resulted in insufficient cellular yield and differentiation. On the other hand, encapsulation of undifferentiated hESCs followed by differentiation induction upon encapsulation resulted in the highest viability and differentiation. More striking was that alginate encapsulation resulted in a much stronger differentiation compared to parallel two-dimensional cultures, resulting in 20-fold increase in c-peptide protein synthesis. To elucidate the mechanism contributing to encapsulation-mediated enhancement in hESC maturation, investigation of the signaling pathways revealed interesting insight. While the phospho-protein levels of all the tested signaling molecules were lower under encapsulation, the ratio of pSMAD/pAKT was significantly higher, indicating a more efficient signal transduction under encapsulation. These results clearly demonstrate that alginate encapsulation of hESCs and differentiation to islet-cell types provides a potentially translatable treatment option for type 1 diabetes.

Introduction

It is well known that type 1 diabetes constitutes ~5–10% of all diabetes cases, wherein the immune system destroys the insulin-producing β-cells of the pancreas.[1] Success of the Edmonton protocol has established islet transplantation as a promising diabetes therapy.[2] However, as with any other organ transplantation, with islet transplantations, patients were still required to be on regular immunosuppression treatments. As an alternative strategy, encapsulation of islets has been proposed to overcome the need for immunosuppressants. The encapsulation systems utilize materials that are permeable enough to allow the diffusion of glucose and other nutrients to the islets, and the diffusion of waste and insulin away from the islets, while masking the islets from the host immune response.[3–6] Alginate is a chemically inert nondegradable polymer, and most importantly it has the capability to immunoisolate encapsulated cells.[7] A simple and commonly used method to ensure whether alginate encapsulation provides sufficient immunoisolation for many cell types is the application of a polycationic coating, followed by an alginate coating.[8–10] These characteristics make it an ideal encapsulation system for islet transplantation, and thus it has been utilized for this purpose for decades.[11–19] Although these methods of transplantation isolate the islets from the host immune response, this treatment option is plagued by shortage of donor islets. Specifically, approximately two to three pancreata worth of islets are necessary to return a diabetic patient to normoglycemia.[20]

A promising alternative to the whole organ or islet transplantation is the use of human embryonic stem cells (hESCs). Pluripotent stem cells have the potential to differentiate to any cell type in the body and are also in virtually unlimited supply, rendering hESC-derived islet-like cells a promising alternative to islets. Previous studies have focused on the induction of islet-like cells from hESCs primarily on the two-dimensional (2D) monolayer platform of tissue culture plastic (TCP).[21–24] While these studies have been successful in deriving insulin-producing cells from embryonic stem cells, they are not directly scalable or translatable for type 1 diabetes treatment. The focus of our study, thus, is to establish the feasibility of obtaining encapsulated hESC-derived islet-like cells, which can be directly transplanted for diabetes therapy. While immunoisolation is the primary advantage of islet encapsulation, it offers the additional advantage of

Departments of [1]Chemical Engineering and [2]BioEngineering, University of Pittsburgh, Pittsburgh, Pennsylvania.

scalability for hESC-derived islets. The high throughput of encapsulation systems will allow the capability of producing the enormous number of pseudo-islets needed for tissue engineering applications.

Encapsulation of embryonic stem cells has been an active area of research over the last decade. The majority of the efforts, however, had been restricted to mouse embryonic stem cells (mESCs) and its differentiation to various cell types.[25–27] Since platforms established for mESCs cannot be directly translated to hESCs, targeted platforms need to be developed to handle issues associated with hESC encapsulation. Siti-Ismail *et al.*[28] have recently shown the feasibility of propagating hESCs encapsulated in calcium alginate for up to a period of 260 days. The encapsulated hESCs were reported to retain their characteristic pluripotency, and could be further induced to each specific germ layer. In another report, Chayosumrit *et al.*[29] have shown the feasibility of inducing definitive endoderm (DE) in encapsulated hESCs. Dean *et al.*[30] have shown that encapsulation of hESCs could prevent teratoma formation for up to 4 weeks after implantation into mice. Finally, Kim *et al.*[31] have used alginate encapsulation for differentiation of hESCs to midbrain dopamine-producing neurons. These initial studies clearly establish the potential benefits in encapsulating hESCs and demonstrate the feasibility of inducing early differentiation in these encapsulated hESCs. There have been no reports to date, however, to the best of our knowledge on exploiting encapsulation strategies for achieving late-stage differentiation of hESCs to the pancreatic lineage. The objective of the current work is thus to demonstrate for the first time the feasibility of generating hESC-derived islet-like cells under alginate encapsulation, which can be readily transplanted for diabetes therapy.

In our previous studies we have reported directed differentiation of hESCs to pancreatic islet cell types in 2D culture consisting of the following stages: DE, pancreatic progenitor (PP), and maturation (MAT).[32] Translation of this protocol into a three-dimensional (3D) encapsulation configuration first requires determination of the specific stage of differentiation when the hESCs can be encapsulated. Our study has shown that encapsulation of undifferentiated (UD) hESCs followed by the stage-wise differentiation successfully results in islet-specific maturation. Further, the maturation obtained under encapsulation was significantly stronger than parallel differentiation conducted in the conventional 2D configuration. We have also evaluated the possibility of encapsulating partially and fully differentiated hESCs. Encapsulation of hESC-derived DE cells resulted in high maturation upon further differentiation; however, the viability of the cells was significantly lower than encapsulating UD hESCs. Encapsulation of hESC-derived mature cells resulted in both low viability and reduction of the maturation markers upon culture. Hence these results show that the stage of encapsulation greatly affects the translation of this protocol. We have further investigated the mechanisms mediating this enhanced maturation under encapsulation and determined that extracellular matrix (ECM) molecules or adhesive molecules may not be mediating the process. On the other hand, investigation of the involved signaling pathways revealed that while the magnitude of key protein expression was low under encapsulation, the ratio of pSMAD/pAKT was significantly higher than the corresponding 2D cultures, indicating the encapsulation strategy as being an efficient approach enhancing differentiation.

Materials and Methods

Cell culture

UD H1 hESCs were maintained on hESC-qualified Matrigel (BD Biosciences)–coated tissue culture plate for 5–7 days in mTeSR1 (StemCell Technologies) at 37°C and 5% CO_2 before passaging. Experiments were performed with p55–p70 hESCs.

hESC encapsulation

Single-cell suspension of UD or predifferentiated hESCs was encapsulated according to previous studies.[29,33] hESCs were incubated with 10 μM Y-27632 (Millipore) for 2 h prior to passaging. Cells were incubated with Accutase (Life Technologies) for 5–7 min at 37°C to detach cells, and pipetted to obtain single cell. Cells (1×10^6 cells/mL) were suspended in filtered 1.1% (w/v) low-viscosity alginate (Sigma-Aldrich) with 0.2% (v/v) gelatin (Sigma-Aldrich) and added drop-wise to a solution of 100 mM $CaCl_2$ (Sigma-Aldrich) with 10 mM HEPES (Sigma-Aldrich) using a 22-gauge needle. The resulting capsules were 1.98 ± 0.14 mm in diameter. The alginate used for encapsulation consisted of 39:61 guluronic to manuronic acid residues and an endotoxin content of ~ 88 EU/g.[34] Alginate capsules were incubated for 6–8 min in the $CaCl_2$ solution. Capsules were washed three times with phosphate-buffered saline (PBS) and suspended in appropriate medium with 10 μM Y-27632 for 4 days prior to differentiation.

Differentiation of encapsulated hESCs

The stage-wise induction protocol for mature islet-like differentiation of hESCs was adopted from our previous study.[32] First, DE was induced using 100 ng/mL ActivinA (R&D Systems) with 25 ng/mL Wnt3A (R&D Systems) for 4 days. Afterward, PP was induced with 0.2 μM KAAD-cyclopamine (Millipore) for 2 days and 0.2 μM KAAD-cyclopamine with 2 μM retinoic acid (Sigma-Aldrich) for 2 days. Finally, maturation was induced by 10 μM nicotinamide (Sigma-Aldrich) for 2 days and 10 μM nicotinamide with 30 μM DAPT (Santa Cruz Biotechnology) for 7 days. All differentiation media were made using DMEM/F12 (Life Technologies), supplemented with 0.2% bovine serum albumin (BSA; Sigma-Aldrich) and 1xB27® (Life Technologies).

Viability

LIVE/DEAD (Life Technologies) viability assay was performed according to manufacturer's instructions. Briefly, encapsulated cells were incubated with 2 μM ethidium homodimer-1 and 1 μM calcein-AM in DMEM/F12 for 25 min at room temperature. Capsules were washed three times with PBS before fluorescent imaging.

Proliferation

Cell proliferation was measured using AlamarBlue (Life Technologies) assay according to manufacturer's instructions.

Briefly, encapsulated cells were incubated with medium containing 10% (v/v) AlamarBlue for 4 h. Fluorescence intensity of the supernatant was measured using a Synergy 2 multimode Microplate Reader (BioTek).

Quantitative real-time polymerase chain reaction

Cells were decapsulated with 100 mM EDTA (Sigma) and washed twice with PBS before lysis. mRNA was isolated using the NucleoSpin RNA II kit (Macherey-Nagel). cDNA was obtained using the ImpromII Reverse Transcription System (Promega). Each polymerase chain reaction (PCR) contained 5 μL SYBR Green Master Mix (Agilent), 2 μL nuclease-free H_2O, 2 μL primer, and 1 μL cDNA. Samples were normalized to the house-keeping gene GAPDH and analyzed relative to UD hESCs using the ΔΔCt method. For the RT^2Profiler™ PCR array analysis, cDNA was obtained using the RT^2 First Strand kit according to manufacturer's instruction (SA Biosciences). Each qRT-PCR for the ECM and adhesion molecule array (human) contained 12.5 μL RT^2 qRT-PCR Master Mix, 0.94 μL cDNA, and 11.56 μL RNase-free water and was distributed (25 μL) into each well of the PCR 96-well array. Encapsulated samples were normalized to the house-keeping gene GAPDH and analyzed relative to hESCs differentiated on TCP using the ΔΔCt method. Gene expression was measured with quantitative real-time polymerase chain reaction (qRT-PCR) using an MX3005P system (Agilent).

MagPix

Intracellular expression of the proteins c-peptide and glucagon was measured by MagPix analysis using the BioPlex Pro Human Diabetes kit (Bio-Rad) according to the manufacturer's instructions. Briefly, samples and standards were incubated with 1× c-peptide and glucagon-labeled magnetic beads at room temperature for 1 h. All incubation steps were done on plate shaker at 300 rpm. After incubation, the beads were washed and incubated with a 1× biotinylated detection antibody solution at room temperature for 30 min. Next, the beads were washed and incubated with 1× streptavidin-PE for 15 min at room temperature. The transforming growth factor β (TGFβ) pathway was analyzed using the MILLIPLEX MAP TGFβ Signaling Pathway Magnetic Bead 6-Plex (Millipore) for pSMAD2, pSMAD3, pERK1/2, and pAKT as well as total TGFβIIR and SMAD4 according to manufacturer's instruction. Briefly, 25 μL of each control and sample was incubated with 25 μL of a 1× beads solution overnight at 4°C. After incubation, the beads were washed twice and incubated with 1× detection antibody for 1 h in the dark, followed by 1× streptavidin-PE for 15 min. Fluorescence intensity was measured using the xMAP (Luminex) machine. The total protein was measured using a BCA total protein kit (Thermo Scientific), according to manufacturer's instruction.

Glucose-stimulated hormone release

After mature differentiation of UD-encapsulated hESCs, cells were incubated overnight in low-glucose (2.8 mM) differentiation media containing 10 μM nicotinamide. Next, the cells were included for 1 h in Krebs-Ringer buffer at 37°C followed by a 1- or 3-h stimulation with high-glucose (16.7 mM) differentiation media containing 100 μM tolbutamide and 30 μM KCl. Levels of secreted glucagon and c-peptide in the supernatant were measured at basal conditions (low glucose) and after stimulation using MagPix analysis as previously described. Secreted hormones were normalized to the total protein of the stimulated cells.

Western blot

Cell lysis was carried out in Cell Extraction Buffer (Invitrogen) by incubation with cells on ice for 30 min, followed by centrifugation for 30 min at 3220 *g* at 4°C. Proteins (30 μg per sample) were separated using 4–20% SDS-PAGE at 100 V, and were transferred to nitrocellulose membrane at 4°C overnight. The membrane was blocked with Odyssey blocking buffer (LI-COR Biosciences) for 2 h at room temperature. Primary antibodies against β-Catenin (1:1000; Cell Signaling), and GAPDH (1:5000; Cell Signaling) were diluted in Odyssey blocking buffer with 0.1% tween (Sigma-Aldrich) and were added to the membrane and incubated overnight at 4°C. The membrane was washed three times for 5 min each and incubated with IR-conjugated anti-rabbit secondary antibody (1:20,000; LI-COR) for 1 h at room temperature. The membrane was washed three times for 5 min each before analysis using the Odyssey CLx (LI-COR) machine. Samples were normalized with GAPDH values.

Flow cytometry

Cells were harvested after Accutase treatment to obtain a single-cell suspension, and were fixed with 4% formaldehyde (Thermo Scientific) in PBS for 30 min. Cells were permeabilized with 0.1% Saponin (Sigma-Aldrich) with 0.5% BSA in PBS for 30 min. Blocking for nonspecific binding was done by incubating cells with 3% BSA with 0.25% dimethyl sulfoxide and 0.1% Saponin in PBS for 30 min. Samples were incubated in blocking buffer with rabbit anti-c-peptide (1:500; Abcam) primary antibody for 30 min at room temperature. Next, cells were incubated with donkey anti-rabbit Alexafluor 555 (Life Technologies) for 30 min at room temperature. Secondary anti-only with primary antibody was used as the negative control. Samples were washed and suspended in PBS before transferring to flow cytometry tubes. Accuri C6 © Flow Cytometer was used to quantify the protein expression. The gate was set beyond cells positive for secondary antibody only to eliminate false positives.

Immunostaining

Encapsulated cells were fixed with 4% formaldehyde for 30 min. Cells were dehydrated with increasing concentrations of ethanol and paraffin embedded for sectioning. Antigen retrieval was done using citrate buffer. Slides were permeabilized with 0.1% Triton-X (Sigma) in PBS for 5 min. A blocking step with 10% donkey serum in PBS was done for 1 h. For primary antibodies, we used goat anti-SOX17 (1:200 dilution; Santa Cruz Biotechnology), rabbit anti-FOXA2 (1:200 dilution; Santa Cruz Biotechnology), goat anit-PDX1 (1:50 dilution; R&D Systems), rabbit anti-c-peptide (1:500 dilution), goat anti-glucagon (1:200 dilution; Santa Cruz Biotechnology), rabbit anti-MAFA (1:500 dilution; Bethyl Laboratories), and mouse anti-somatostatin

(1:200; Beta Cell Biology Consortium). The incubation time for primary antibodies was overnight at 4°C. The slides were incubated with the secondary antibody for 45 min at room temperature. Secondary antibodies used were as follows: donkey anti-rabbit Alexafluor 555 (1:500 dilution), anti-goat Alexafluor 555 (1:500 dilution), and anti-mouse Alexafluor 488 (1:500 dilution). The slides were washed three times with PBS (5–10 min) before covering with hardening mounting medium containing DAPI (Vectashield; Vector laboratory).

Statistical analysis

Data were presented as mean ± SD. Statistical significance between groups was determined using the two-tailed Student's *t*-test for two-group comparisons. Probability values at $*p < 0.05$ and $**p < 0.01$ indicated statistical significance.

Results

Pancreatic differentiation of hESCs

We have previously reported a stage-wise directed differentiation protocol for induction of hESCs to mature islet-like cell types[32] on conventional 2D monolayer TCP. Figure 1A shows our protocol for islet-like differentiation of hESCs, which consists of the following stages: DE, PP, and MAT. A single-cell suspension of UD hESCs or predifferentiated hESCs was dispersed in 1.1% alginate with 0.2% gelatin, and added drop-wise to a bath of $CaCl_2$ (Fig. 1B).

Encapsulation of predifferentiated hESCs results in low yield of viable cells

Characterization of predifferentiated cells. Calcium alginate encapsulation has been commonly used to immunoisolate islets from the host immune response. Thus, our first objective was to investigate the possibility of calcium alginate encapsulation of predifferentiated hESCs either after full maturation or upon DE induction, and test the viability and functionality upon encapsulation. UD hESCs were first induced to mature or DE cells on Matrigel-coated TCP using the previously described differentiation protocol, and encapsulated in alginate. The mature stage was characterized by upregulation of insulin ($\sim 9.5 \times 10^5$; Fig. 2A) by qRT-PCR, as well as flow cytometry and immunostaining for c-peptide (Fig. 2B, C). Our differentiation protocol yielded $\sim 24\%$ of the population positive for c-peptide by flow cytometry. Before encapsulation of DE cells, differentiation in 2D was confirmed by analysis of DE markers by qRT-PCR (Supplementary Fig. S1A; Supplementary Data are available online at www.liebertpub.com/tea), flow cytometry (Supplementary Fig. S1B), and immunohistochemistry (Supplementary Fig. S1C). Encapsulated mature cells were maintained for 7 days in basal maturation media (B27, BSA, and nicotinamide), while encapsulated DE cells were further differentiated according to Figure 1A.

Viability and proliferation. The viability of encapsulated islet-like cells was analyzed on days 1, 3, and 7

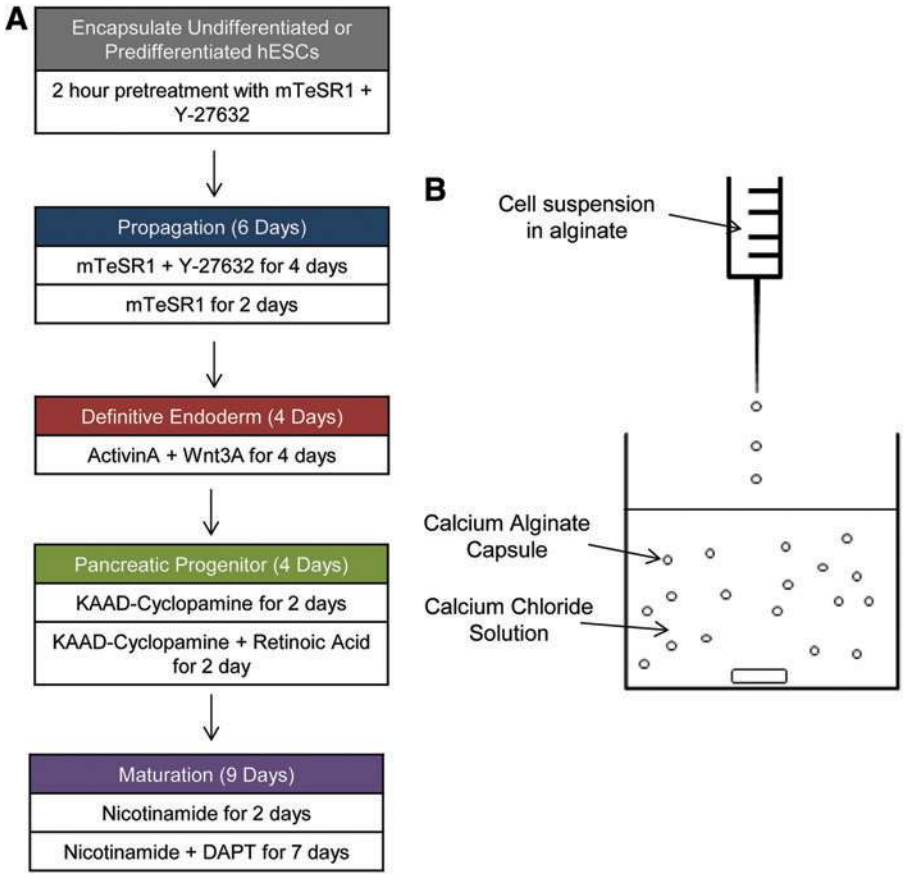

FIG. 1. Experimental setup and stage-wise differentiation protocol. **(A)** Stage-wise differentiation protocol for deriving mature islet-like cell types from hESCs. **(B)** Schematic showing the process of calcium alginate encapsulation of hESCs. hESCs, human embryonic stem cells. Color images available online at www.liebertpub.com/tea

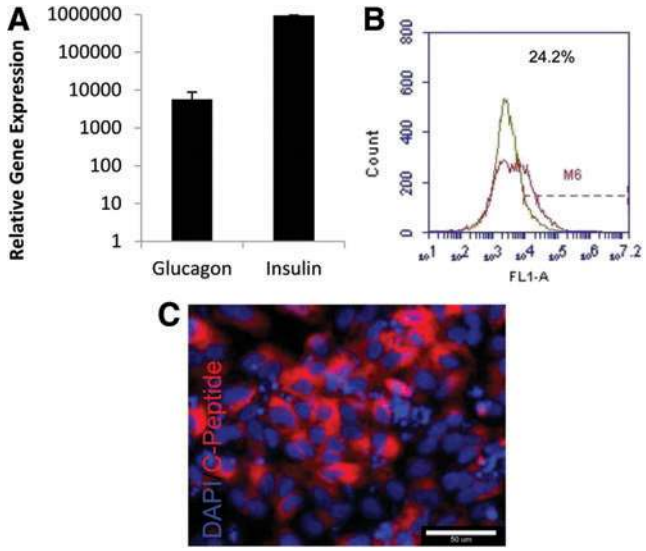

FIG. 2. Characterization of mature islet-like cells before encapsulation. **(A)** Gene expression by qRT-PCR at the mature stage on tissue culture plastic (TCP) for glucagon and insulin, compared with undifferentiated (UD) hESCs ($n=3$). **(B)** Flow cytometry analysis for c-peptide on hESC-derived mature cells on TCP. Secondary antibody only was used as negative control. **(C)** Immunostaining analysis for c-peptide on hESC-derived mature cells on TCP. qRT-PCR, quantitative real-time polymerase chain reaction. Color images available online at www.liebertpub.com/tea

postencapsulation, using the LIVE/DEAD assay (Supplementary Fig. S2). Figure 3A shows images from days 1 and 7. Viable cells fluoresce green by metabolically converting calcein-AM to calcien, while the dead cells fluoresce red by diffusion of ethidium-homodimer-1 into the cell due to the permeability of apoptotic cells. Day-1 bright field and fluorescent images confirm the presence of live cells in the alginate capsule, indicating successful encapsulation of the hESC-derived islet-like cells. Apoptotic single cells were also observed in the alginate capsules, which are expected due to the increased stress on the cells during harvesting and encapsulation. The hESC-derived mature cells are, however, not strongly proliferative. Hence, the number of viable cells in the alginate capsules remains unchanged throughout the 7 days of culture. Consequently, colony formation was not observed and the yield of the viable, encapsulated cells was low.

Viability and proliferation of encapsulated DE cells was analyzed at the end of each stage of the differentiation, after encapsulation (Supplementary Fig. S3A, B). Figure 3B shows that although beyond day 7, cellular aggregation into small colonies was observed, the size of these colonies did not increase appreciably by the end of maturation as shown by the LIVE/DEAD images on day 14. Although the yield of the viable cells is higher compared with encapsulating mature cells, the overall yield of viable cells is still low.

Effect of encapsulation on hESC maturation. The encapsulated mature cells were further analyzed for mature pancreatic markers after 7 days of culture to verify whether the encapsulated cells maintained their differentiated phenotype. Differentiated cells analyzed at the point of encapsulation showed strong upregulation of *PDX1* (51-fold), glucagon (5635-fold), and insulin (9.5×10^5-fold). This condition was used as a positive control. Upon culture under encapsulation, the cells still retained their maturation markers: *PDX1* ($\sim$3-fold), *MAFA* ($\sim$19-fold), glucagon ($\sim$1309-fold), and insulin ($\sim4.8\times10^5$-fold) (Fig. 3C). However, the strength of upregulation was reduced with culture; expression of *PDX1*, glucagon, and insulin showed, respectively, 18.6, 4.3, and 19.6-fold lower upregulation after 7 days under encapsulation. This indicates that, while it is feasible to encapsulate hESC-derived islet-like cells, the cells tended to lose their mature phenotype upon encapsulation.

Analysis of the encapsulated DE cells after pancreatic induction shows strong upregulation of *PDX1* gene expression, a crucial transcription factor in pancreatic development (Supplementary Fig. S3C). The encapsulated hESC-derived DE cells were further matured into islet-like cells, and analyzed for the gene expression of more mature pancreatic islet markers. As illustrated in Figure 3D, maturation of encapsulated cells resulted in strong upregulation of many of the mature markers: *PDX1* ($\sim$2500-fold), glucagon ($\sim2.5\times10^5$-fold), *MAFA* ($\sim$14-fold), and insulin ($\sim2.5\times10^6$-fold) compared with UD hESCs. *PDX1* and insulin expression was, respectively, 50- and 2.8-fold higher upon encapsulation, compared with 2D TCP controls. These results indicate the enhanced pancreatic potential of the hESC-derived DE cells upon encapsulation. However, although encouraging as a differentiation platform, the just-discussed configuration is restrictive for cellular yield.

Encapsulation of UD hESCs results in high viability and strong islet-specific maturation

The previous analysis indicated the difficulty in encapsulating predifferentiated hESCs, but it established the positive attribute of encapsulation on differentiation. Hence in the next step, we evaluated the feasibility of encapsulating UD hESCs and conducting all the stages of differentiation under encapsulation. UD hESCs were pretreated with Y-27632 for 2 h, harvested, and encapsulated in alginate. Upon encapsulation, the cells were further propagated for 4 days in mTesR1 with Y-27632, followed by 2 days in only mTeSR1, to allow colony formation. After propagation, the encapsulated cells were induced toward differentiation according to the previously described protocol (Fig. 1A).

Viability and proliferation. Viability and proliferation of UD-encapsulated cells were assessed by LIVE/DEAD and AlamarBlue assays throughout the differentiation protocol. Some apoptotic single cells were observed immediately after encapsulation (Fig. 4A), but the apoptotic cell population did not increase even after 23 days of encapsulation. Unlike previous encapsulation configurations, small cell colonies were visible after the propagation stage, which continued to grow into large viable colonies by the end of maturation. The vast majority of the cells in the individual colonies remained viable after maturation, although some apoptotic cells were observed on the periphery of colonies toward the end of maturation. Figure 4B shows proliferation of encapsulated hESCs, represented as fluorescence intensity per capsule. Proliferation of encapsulated cells progressively increased up to the end of PP stage, and decreased slightly after maturation. These results clearly

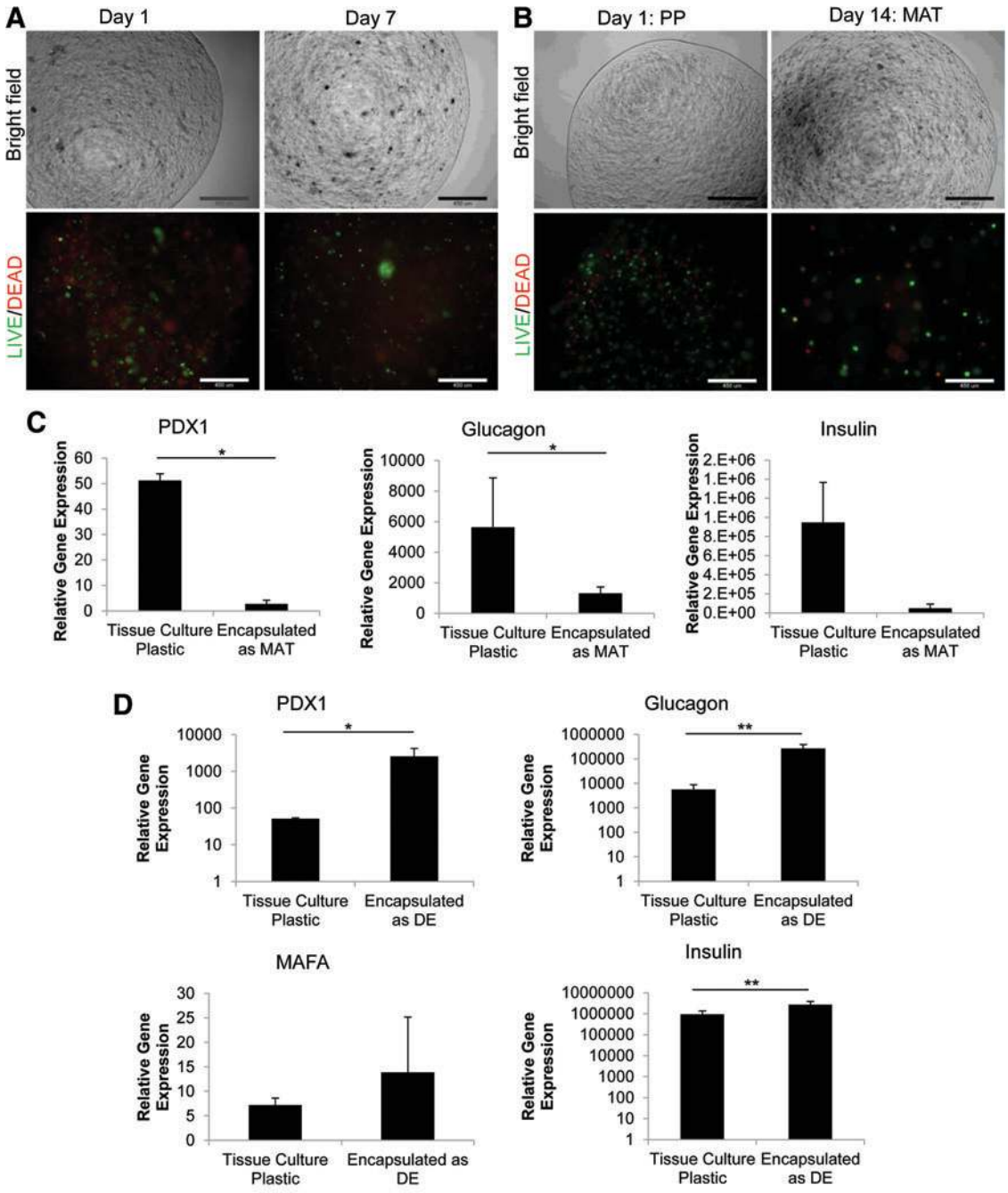

FIG. 3. Characterization of encapsulated predifferentiated hESCs. **(A)** LIVE/DEAD viability assay on days 1 and 7 after encapsulation of hESCs matured to islet-like cells on TCP. **(B)** LIVE/DEAD viability assay on days 1 and 14 after encapsulation of hESC-derived definitive endoderm cells. **(C)** Gene expression by qRT-PCR on islet-like cells, 7 days postencapsulation, for *PDX1*, glucagon, and insulin, compared with UD hESCs ($n=3$). 2D TCP controls represent the cell population prior to encapsulation. **(D)** Gene expression by qRT-PCR at the mature stage on cells encapsulated at the definitive endoderm (DE) stage, for *PDX1*, glucagon, *MAFA*, and insulin. TCP controls are hESCs that were differentiated to islet-like cells entirely on TCP. The results were considered significant if $*p<0.05$, $**p<0.01$ ($n=3$). Scale bar is 450 μm. Color images available online at www.liebertpub.com/tea

indicate a significant increase in the cellular viability and overall yield of mature cells by encapsulating UD hESCs rather than predifferentiated hESCs.

Differentiation under encapsulation. Having confirmed high viability of the encapsulated hESCs, the next question is the differentiation potential of the encapsulated cells. Cellular differentiation was analyzed in detail after each stage of the induction protocol by using stage-specific markers. Gene expression analysis after DE induction of the encapsulated hESCs showed strong upregulation of the DE markers *SOX17* (~400-fold), *FOXA2* (~90-fold), *CXCR4*

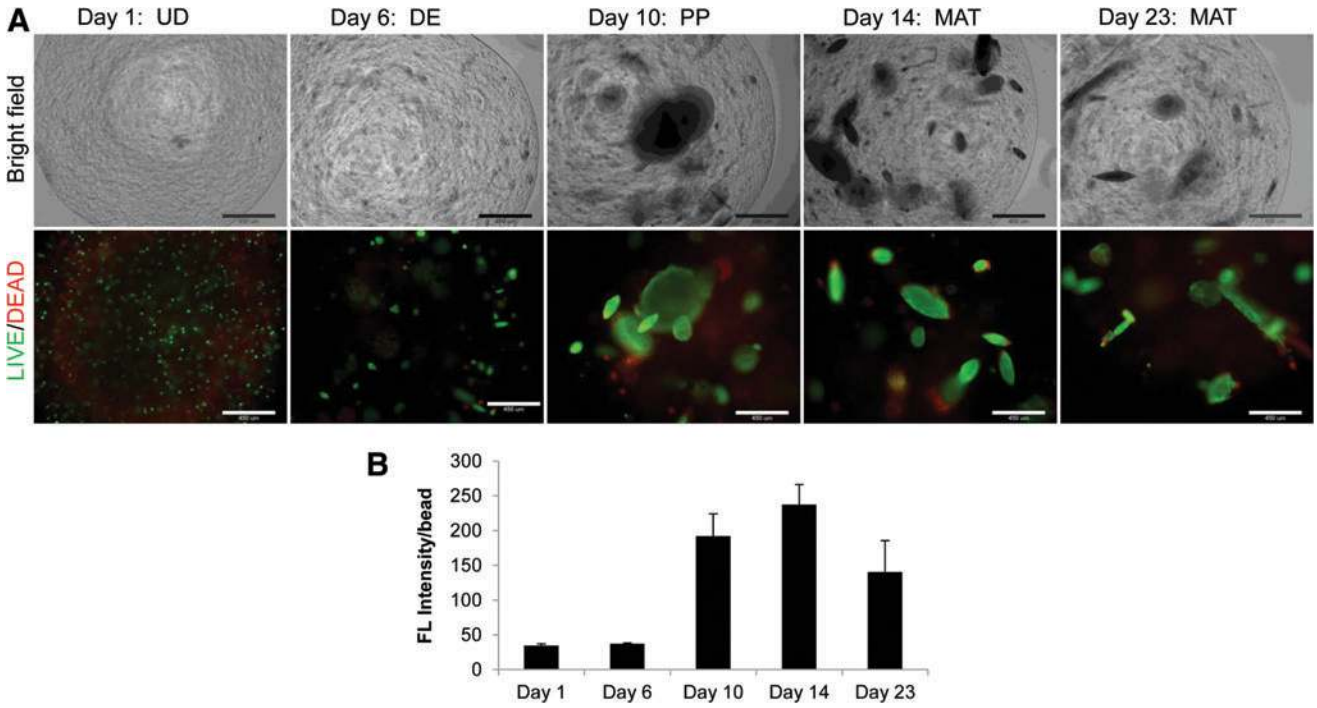

FIG. 4. Viability and proliferation of hESCs encapsulated at the UD stage. **(A)** LIVE/DEAD viability assay on the first and last days of differentiation, for each stage after encapsulation. **(B)** AlamarBlue proliferation assay on the first and last days of differentiation, for each stage after encapsulation ($n=3$). Scale bar is 450 μm. Color images available online at www.liebertpub.com/tea

(~72-fold), and *CER* (~175-fold) compared with UD hESCs (Fig. 5A). All these DE markers were found to be upregulated under encapsulation, although the levels were not significantly different from parallel 2D controls. Analysis of protein expression using immunostaining confirmed SOX17- and FOXA2-positive cells in the encapsulated cells (Fig. 5B). These findings indicate successful induction of encapsulated hESCs to the DE stage.

The next step was analysis of the PP stage. Similar to DE, the PP stage also showed strong upregulation of *PDX1* when encapsulated, showing ~3000-fold increase compared with UD hESCs (Fig. 5C), which was folds higher than parallel 2D controls. Immunofluorescence analysis showed colonies of encapsulated cells strongly positive for the PDX1 protein (Fig. 5D), confirming differentiation to the PP stage.

The encapsulated cells were further induced toward islet maturation as detailed in Figure 1A. Maturation was achieved by notch inhibition by addition of DAPT for 7 days. At the end of the entire protocol the encapsulated cells were analyzed for mature pancreatic islet-specific markers. Gene expression analysis at the mature stage showed strong upregulation of the beta cell markers insulin (~8×10^5-fold) and *MAFA* (14-fold), as well as the alpha cell marker glucagon (~3×10^4-fold), compared with UD hESCs (Fig. 6A). Unlike the previous stages, the strength of the mature markers under encapsulation was comparable to that of the control in conventional 2D cultures. The exception to this is *PDX1* (800-fold), which was several folds stronger than parallel TCP controls, although this difference was not significant. Detailed immunostaining characterization of the encapsulated cells revealed cell colonies positive for PDX1, as well as MAFA, which has been implicated in the mechanism of glucose-responsive insulin secretion (Fig. 6B). Additionally, cells were positive for glucagon and somatostatin, as well as a considerable number of cells were positive for c-peptide, all of which are hormones secreted by islets (Fig. 6B). While some of the cells were polyhormonal, expressing both c-peptide and glucagon as shown in Supplementary Figure S4A, there were distinct populations of cells expressing single hormones (Supplementary Fig. S4B). Thus, differentiation of encapsulated UD cells shows a high cellular yield as well as efficient differentiation to mature pancreatic phenotype, as indicated by gene and protein expression of mature pancreatic islet markers.

Intracellular C-peptide and glucagon content and release

As a final analysis of the maturation of hESC-derived islet-like cells, we measured the intracellular protein content and protein secretion of the islet-specific hormones c-peptide and glucagon, shown in Figure 7. Mature insulin is produced by post-translational cleavage of proinsulin into insulin and c-peptide. Thus, intracellular c-peptide content is analogous to intracellular insulin, and is a measure of avoiding any artifacts arising from insulin in the culture media. Quantification of the intracellular c-peptide and glucagon protein content was performed using Luminex-based MagPix assay. The encapsulated UD hESCs were found to contain 0.39 pg c-peptide/μg total-protein, which was 20-fold higher than the 2D controls, containing 0.019 pg c-peptide/μg total-protein. Similarly, the encapsulated UD

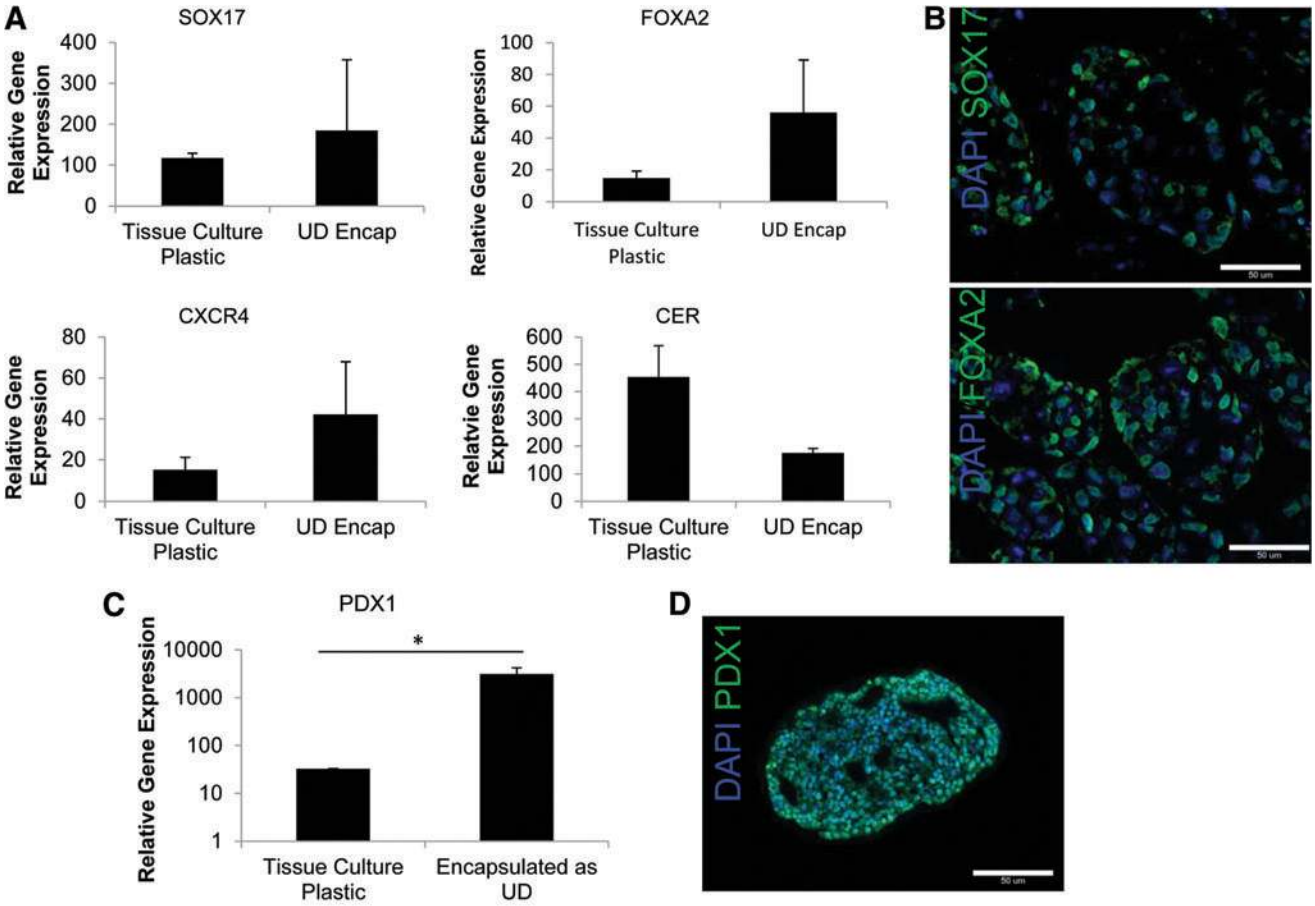

FIG. 5. Characterization of the definitive endoderm and pancreatic progenitor stage for hESCs encapsulated at the UD stage. **(A)** Gene expression by qRT-PCR at the definitive endoderm stage for *SOX17*, *FOXA2*, *CXCR4*, and *CER*, compared with UD hESCs ($n=3$). **(B)** Immunostaining at the definitive endoderm stage for SOX17 and FOXA2. **(C)** Gene expression at the pancreatic progenitor for *PDX1* stage after encapsulation, compared with UD hESCs ($n=3$). **(D)** Immunohistochemistry at the pancreatic stage for PDX1. Scale bar is 50 μm. The results were considered significant if $^*p<0.05$. Color images available online at www.liebertpub.com/tea

hESCs showed 0.085 pg glucagon/μg total-protein, while 2D showed 0.006 pg glucagon/μg total-protein (Fig. 7A).

After confirming the ability of hESC-derived cells to synthesize islet-specific hormones, we wanted to evaluate the mature functionality of the cells in sensing and responding to extracellular glucose with enhanced insulin/c-peptide release. The presence of potassium channel K_{ATP} required for c-peptide release was confirmed by the upregulation of the K_{ATP} subunit genes *KIR6.2* and *SUR1* (Fig. 7B). Glucokinase, a key molecule involved in sensing glucose levels, also showed an upregulation in gene expression (Fig. 7B). Finally, we analyzed the release of c-peptide in response to stimulation for 1 and 3 h with physiologically relevant high glucose concentration (16.7), tolbutamide, and KCl. Upon stimulation for 1 and 3 h, the mature islet-like cells released 0.008 and 0.031 pg c-peptide/μg total-protein into the media, respectively (Fig. 7C). Stimulation resulted in ~1.5-fold and 3.9-fold higher c-peptide release over the basal conditions for 1 and 3 h stimulation, respectively. Thus, it can be construed that hESC differentiation under alginate encapsulation promotes both hormone synthesis and release in response to stimulation.

Enhanced differentiation is likely due to increased pSmad/pAKT ratio

Since encapsulated differentiation of hESCs enhanced its maturation over the conventional 2D TCP control, we further investigated the cause of these enhancements. Our initial hypothesis was that the ECM and cell adhesion molecules (CAM) in the encapsulated cell clusters are mediating this process. Hence we first analyzed the global gene expression of ECM and CAM molecules for both the 2D cultures and encapsulated cultures at the DE and PP stages using the ECM and adhesion molecule array. This array profiles genes important for cell–cell adhesion, cell–matrix adhesion, and various ECM molecules. Figure 8A shows the results for this gene array represented as a heatmap, for CAM, ECM, and molecules categorized as both CAM and ECM (BOTH). The heatmap represents relative gene expression of encapsulated cells at DE and PP stages, compared with the 2D control evaluated at DE and PP stages, respectively. Overall we observed that most of the tested molecules were either unchanged at the DE stage or downregulated, while the PP stage showed a more prominent

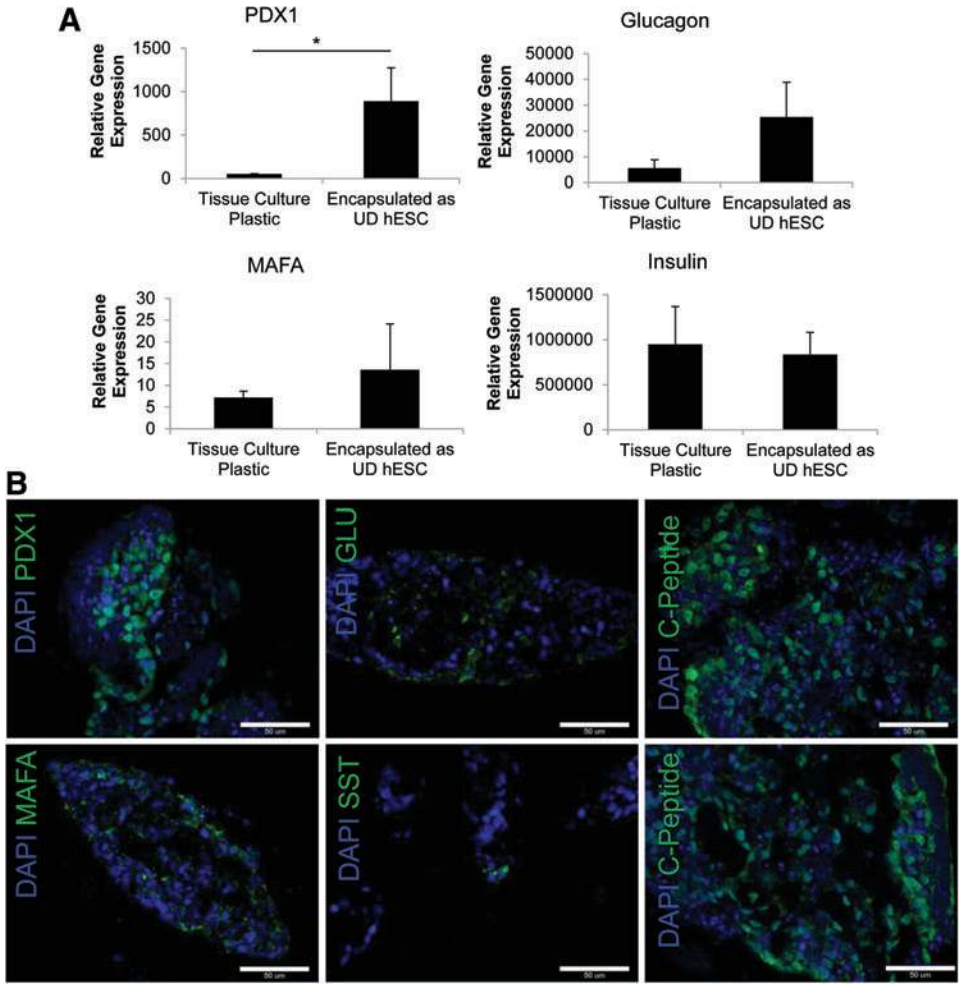

FIG. 6. Characterization of mature islet-like cells, encapsulated as UD hESCs. **(A)** Gene expression of the mature markers *PDX1*, glucagon, *MAFA*, and insulin, compared with UD hESCs ($n=3$). **(B)** Immunohistochemistry at the mature stage for PDX1, glucagon (GLU), MAFA, somatostatin (SST), and c-peptide. Scale bar is 50 µm. The results were considered significant if $*p<0.05$ ($n=3$). Color images available online at www.liebertpub.com/tea

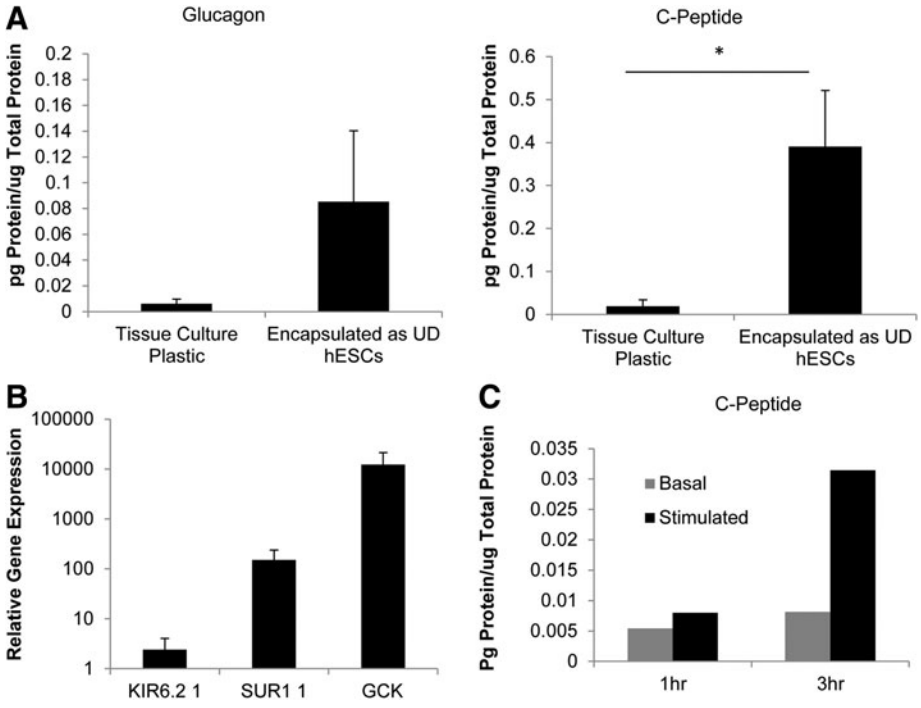

FIG. 7. Intracellular protein quantification and glucose sensing. **(A)** Intracellular c-peptide and glucagon content at the mature stage for UD-encapsulated hESCs, measured by MagPix analysis. **(B)** Gene expression analysis of the glucose-sensing molecules *KIR6.2* and *SUR1* (subunits of K_{ATP} channel) and glucokinase (*GCK*) at the mature stage for UD-encapsulated hESCs. **(C)** Released c-peptide in response to basal conditions (low glucose) and after stimulation with high glucose (16.7 mM), 100 mM tolbutamide, and 30 mM KCl for 1 and 3 h, respectively, measured by MagPix analysis. The results were considered significant if $*p<0.05$ ($n=2$).

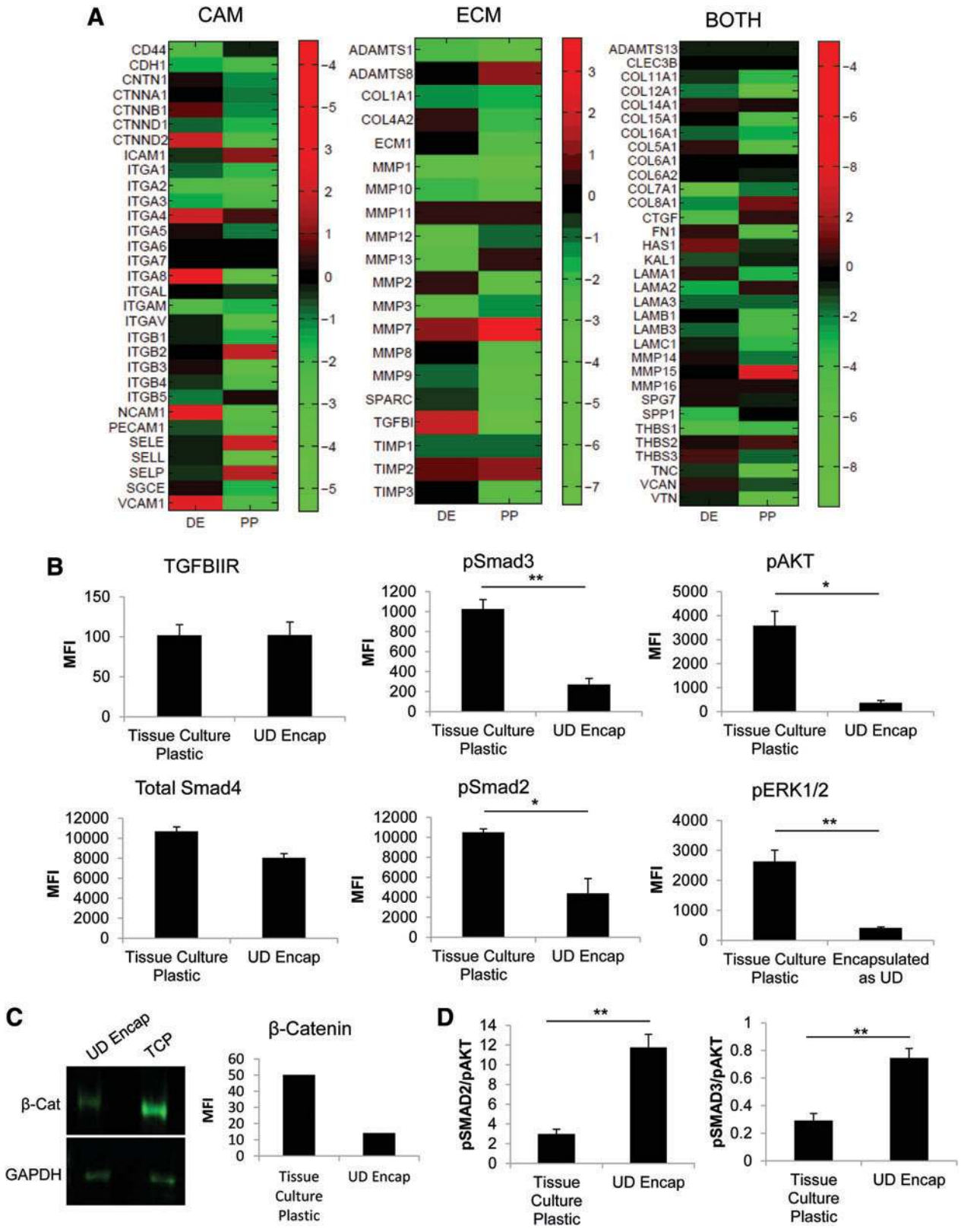

FIG. 8. Characterization of enhanced differentiation for cells encapsulated as UD hESCs. **(A)** Extracellular matrix and adhesion molecule gene expression array by qRT-PCR at the definite endoderm and pancreatic progenitor stage, compared with cells differentiated on TCP. Gene expression fold changes were log2-transformed and are represented as a heatmap. **(B)** Protein expression of key molecules in the TGFβ pathway, and molecules that are known to interact with this pathway by MagPix analysis after definitive endoderm differentiation ($n=3$). **(C)** Western blot analysis for β-catenin, a crucial molecule in the WNT signaling, after definitive endoderm differentiation. MFI is normalized to GAPDH. **(D)** The ratios of pSMAD3/pAKT and pSMAD2/pAKT after definitive endoderm differentiation. The results were considered significant if $*p<0.05$, $**p<0.01$. qRT-PCR, quantitative real-time polymerase chain reaction; TGFβ, transforming growth factor β. Color images available online at www.liebertpub.com/tea

downregulation of the tested molecules under encapsulation. There were only few molecules that were consistently upregulated under both DE and PP conditions, of which *MMP7* had the highest upregulation. *MMP15* was strongly upregulated in PP stage, but was unchanged at DE. Of the CAM molecules, *VCAM1, NCAM1, ITGA8,* and *ITGA4* were strongly upregulated at the DE stage but were downregulated at PP.

Next, we wanted to evaluate the primary signaling pathways mediating the process of differentiation. We concentrated on the DE stage since DE differentiation is critical in achieving successful maturation of the hESCs into functional cell types. Since DE induction was achieved through the activation of TGFβ and WNT pathway, we measured the expression of the primary effectors of these pathways. For TGFβ pathway we focused primarily on expression of key SMAD molecules by Luminex-based MagPix assay, and for WNT pathway we measured expression of β-catenin by western blot analysis. Quite interestingly, we found that the expression level of the key effectors of the pathways—pSMAD2, pSMAD3 (Fig. 8B), and β-catenin (Fig. 8C)—was lower under encapsulation. Additional analysis of the TGFβ pathway showed little-to-no difference under encapsulation compared with 2D culture for *TGFR1*, its coreceptor *crypto*, and the transcription factor *FOXH1* (Supplementary Fig. S5A). Next, we looked at the pathways and molecules that are known to have considerable interactions with the TGFβ and WNT. Analysis of the MAPK pathway showed downregulation of *FGFR1* under encapsulation and in 2D cultures, while its coreceptor *SHB* was slightly upregulated (Supplementary Fig. S5B). With both the *FGF1* receptor and its coreceptor, no difference was observed under encapsulation and in 2D cultures. For the hedgehog pathway, although the difference was not significant, we saw higher upregulation of *SHH* in 2D culture as compared with encapsulation (Supplementary Fig. S5C). *SHH* inhibition is required for PP induction; thus, the lower expression seen under encapsulation after DE differentiation could have resulted in improved PP induction under encapsulation as compared with 2D cultures. Consistent with the other molecules, the expression of pAKT and pERK was also found to be lower under encapsulation than in 2D cultures (Fig. 8B). However, low expression of these crosstalk molecules from parallel pathways will be indicative of less influence of negative feedback. To quantify this effect, we evaluated the ratio of pSMAD2 and pSMAD3 with pAKT. It was consistently observed that pSMAD/pAKT ratio was significantly higher under encapsulation compared with TCP cultures (Fig. 8D). This indicates that the increased differentiation observed under encapsulation could be due to an increased ratio of pSMAD2/3/pAKT.

Discussion

In this study we are presenting a detailed procedure for obtaining hESC-derived, encapsulated islet-like cells that can be directly implanted for treatment of the autoimmune disease type 1 diabetes. The presented study will address the shortage for donor islets by providing a platform for high throughput and directly implantable regenerative cell source. Deriving functional islet-like cell types from pluripotent stem cells has the potential for creating a major transformative impact in cell therapy. Hence this has been an intensely researched area over the past decade, with multiple studies including our own investigating pathways for efficient differentiation of hESCs to islet-like cell types on conventional TCP culture configuration.[21,23,24] In contrast to those studies, the current report specifically focuses on deriving encapsulated islet-like cells from hESCs. The criteria for useful encapsulation will be high insulin per bead that needs (1) adequate maturation of the encapsulated cells and (2) high yield of viable encapsulated cells.

In our previous study we have reported a stage-wise differentiation protocol for differentiating hESCs to mature islet-like cell types.[32] In the current study, we further extended our 2D protocol to evaluate for the first time the feasibility and configuration for 3D encapsulation of hESC-derived cell types. The first logical extension of our 2D protocol to a 3D system was to fully differentiate hESCs to mature islet-like cells in 2D, followed by harvesting and encapsulation of these differentiated mature cells. Our results demonstrated that encapsulated cells were initially viable, but their viability decreased with continuous culture. It is known that the proliferation rate of hESCs progressively reduces with differentiation, and typically the cells are not proliferative after maturation. Hence, the cell loss upon encapsulation could not be recovered by the proliferation of the live cells. Further, the encapsulated cells appeared to lose the mature phenotype, as exhibited by the rapid downregulation of mature gene expression of the encapsulated cells. It is difficult to conclude whether the encapsulated cells are going through dedifferentiation, or whether the more mature cells are prone to apoptosis, while the surviving cells are a less-differentiated subpopulation. Alternatively, the disruption of the ECM microenvironment and cell–cell contact formed during the 23-day differentiation protocol during the harvesting step could have led to the low viability of encapsulated cells. Previous studies have also shown that dissociation of islet clusters leads to loss of cell function and apoptosis,[35] possibly indicating that our hESC-derived islet-like cells require cell–cell contact similar to primary islets. Additionally, previous work with islet-like maturation of hESCs by implantation of PPs using the Theracyte device has shown that colony formation is required for development of insulin-producing cells, while single-cell suspensions failed to develop into insulin-secreting cells.[36,37] Thereby an encapsulation strategy ensuring adequate cell–cell contact and cell-cluster formation will be required to ensure functionality upon complete maturation of hESCs.

With the failure to maintain the phenotype of mature cells upon encapsulation, we considered encapsulation of a partially differentiated hESC population that still retains proliferative potential. The hESCs are still proliferative in the DE stage, but proliferation slows down considerably during the induction of the PP stage. Hence we next explored encapsulating predifferentiated DE cells, followed by further pancreatic induction under encapsulation. When we encapsulated hESC-derived DE cells, we saw moderately better viability immediately after encapsulation compared with encapsulation of mature cells. The cells also grew into small cell colonies upon maturation and proliferation of encapsulated DE cells was highest immediately after encapsulation, but decreased by the end of

maturation. This was expected because mature cells are known to show little or very slow proliferation.[38] This, combined with normal apoptosis during differentiation, could explain the decrease in proliferation by the end of maturation. It is unlikely that diffusion limitations from encapsulation were causing any cell death, since the alginate capsule is very porous, and the encapsulated cell aggregates are fairly small in size ($\sim 350\,\mu m$ in diameter). Although DE-encapsulated cells show adequate induction to the mature stage, as well as improved viability, the yield of viable cells is still very low. The transplantation of these encapsulated islet-like cells is volume limited. A low yield of encapsulated viable cells requires an increased volume of capsules to meet insulin requirements. Therefore, it is likely that the number of capsules needed to return to normoglycemia would be too high of a volume for the implantation site. It may be possible to enhance the yield of viable cells by increasing the seeding density. However, compensating for cell death by increasing seeding density may restrict the translational potential of this platform.

In our next configuration we therefore explored the encapsulation of UD hESCs and performing the entire maturation under encapsulation. Our results indeed indicate that when UD hESCs were encapsulated and differentiated to mature islet-like cell types, the yield of viable cells was greatly improved. Distinct viable colonies were visible at the end of maturation, a result that was never achieved by encapsulating predifferentiated cells. This could be attributed to the propagation of the encapsulated cells before induction of differentiation, which could have been permissive to colony formation and establishment of cell–cell contact prior to differentiation. Similar to encapsulation of DE cells, we saw a peak in proliferation when encapsulating UD hESCs at the end of the PP stage and proliferation decreased by the end of the maturation stage. This decrease in proliferation can be attributed to slower proliferation of maturing cells and cells undergoing apoptosis during the differentiation process. Additionally, encapsulated UD hESCs at the mature stage show upregulation of the gene *PDX1*, as well as the mature markers glucagon, *MAFA*, and insulin, confirmed by immunostaining. These results therefore unequivocally demonstrate that alginate encapsulation and differentiation of UD hESCs results in adequate islet-like differentiation, as well as a higher yield of viable cells. While encapsulation of hESC-derived PP cells has been previously proposed as a strategy for implantation,[39] our results indicate the difficulty of encapsulating partially differentiated cells. Thus from a purely differentiation standpoint, it is advantageous to perform the entire differentiation under encapsulation. However, from the standpoint of implantation, it will be advantageous to minimize the period of *in-vitro* culture under encapsulation, prior to implantation. This is to minimize the presence of contaminating antigens from encapsulated dead cells during culture and differentiation. Hence we propose the strategy of decapsulating the differentiated hESCs after maturation, followed by its re-encapsulation in ultrapure, endotoxin-free alginate. These alginate capsules will be further modified with a polycation coating, followed by an alginate coating,[8,17] and implanted immediately.

Since encapsulation and differentiation of UD hESCs appear to meet the requirements of adequate mature differentiation and high yield of viable cells, we conducted further characterization of these cells by analysis of intracellular c-peptide levels to seek further insight into possible mechanisms. C-peptide was measured to avoid any artifacts arising from insulin in the media. Protein quantification using MagPix showed that the encapsulated UD hESCs expressed intracellular c-peptide (0.39 pg/μg total-protein) and glucagon (0.019 pg/μg total-protein). Although a previous study with primary mouse islets showed a c-peptide content of 9.93 ng/μg total-protein,[40] considering the present results are obtained with hESCs, this is indeed an encouraging step toward functional islet-like cell types from hESCs in 3D culture. Gene expression analysis showed that the required machinery necessary for glucose-stimulated insulin release was present by upregulation of the K_{ATP} subunits *SUR1* and *KIR6.2* as well as glucokinase. Additionally, the cells were stimulated for 1 and 3 h to determine c-peptide secretion. Upon stimulation, encapsulated UD hESCs at the mature stage secreted 1.5-fold and 3.9-fold higher c-peptide over the basal conditions for 1 and 3 h stimulation, respectively. It is worth noting that, although gene expression for insulin was similar between 2D controls and encapsulated cells, intracellular c-peptide protein was much higher in encapsulated cells after maturation. However, it is unclear whether differentiation under encapsulation is recruiting more islet-like cells or whether the differentiated cells are eliciting higher levels of gene and protein? This enhancement could be attributed to the 3D environment provided by the alginate encapsulation forcing cell–cell contact, and is thus more closely mimicking the native environment that cells would experience *in vivo*.[41] To investigate this further, we analyzed the gene expression levels of ECM and CAM molecules using a PCR array previously used to analyze the dynamics of embryoid body differentiation.[42] We expected to observe higher levels of CAM expression when comparing traditional 2D culture with our 3D alginate system, since the alginate hydrogel confines the differentiating hESCs. However, the gene array revealed that a large majority of the genes profiled were downregulated with respect to the 2D configuration for both ECM and CAM molecules at both the DE and PP stages. While most of the genes were downregulated, *ITGA4* and *ITGA8* were upregulated at the DE stage, and *MMP7* as well as *MMP15* were however upregulated at the PP stage. *ITGA4* is one of the integrins that encode the subunits of heterodimeric integrin's receptors that bind fibronectin and vitronectin, which are important matrix proteins during DE differentiation.[43] *MMP15* has been shown to be highly expressed in the mature pancreas and *MMP7* to a lesser extent.[44] Next, we evaluated the expression of pSMAD3 and β-catenin, key molecules that directly influence DE differentiation in the TGFβ and WNT pathways, respectively. Surprisingly, the expression of both β-catenin and pSMAD3 was lower in encapsulated cells than in cells on 2D, even though the resultant differentiation initiated by these signaling pathways was significantly higher in encapsulated cells. Hence we analyzed the parallel signaling pathways since the effect of crosstalk has been recently shown to be dominant in differentiating hESCs.[45] pAKT is known to be a strong negative regulator of SMAD3[46,47]; hence, we analyzed the levels of pAKT that was seen to be weaker under encapsulation. It is thus likely that even though the levels of

pSMAD2/3 are higher in 2D cultures, the available proteins for nuclear translocation and hence gene transcription are lower from negative interaction with pAKT. For a more quantitative evaluation, we next evaluated the ratio of pSMAD2/pAKT and pSMAD3/pAKT, both of which were significantly higher under encapsulation compared with 2D cultures. Hence we hypothesize that even though the expression levels of key protein molecules are lower under encapsulation, the signaling cascade is more effective because of reduced negative interactions, as judged by the high levels of pSMAD3/pAKT and pSMAD2/pAKT ratio. This indicates that under encapsulation more SMAD complex is available for translocation to the nucleus, which helps influence the differentiation. While pSMAD/pAKT ratio has been implicated to be critical in TGFβ-induced apoptosis in various different cell types,[46] we report its importance in determining the differentiation potential of hESCs toward the DE cell type.

This research clearly shows that the configurations (stage) in which cells are encapsulated affect their viability/differentiation, and therefore their transplantation potential. We have shown that encapsulation of mature islet-like cells or hESC-derived DE cells resulted in a low yield of viable cells after maturation. Although encapsulation of hESC-derived DE cells showed adequate cellular maturation, encapsulation of UD hESCs was the preferred configuration since it distinctly showed adequate differentiation along with a high yield of viable cells. In fact, we have shown that differentiation of encapsulated UD hESCs resulted in a stronger expression of primary maturation markers and enhanced hormone synthesis compared with parallel 2D cultures. This suggests that encapsulation and mature differentiation of UD hESCs has the highest transplantation potential for treatment of type 1 diabetes. Further, our analysis indicated that the high levels of pSMAD/pAKT ratio obtained upon encapsulation appear to be the primary mediator for differentiation, further validating the promising therapeutic benefits of encapsulation of hESCs in alginate.

Acknowledgments

The project described was supported in part by the National Institutes of Health through Grant numbers UL1 RR024153 and UL1TR000005. The authors acknowledge the Center for Complex Engineered Multifunctional Materials (CCEMM) for providing partial financial support for this research. I.B. also acknowledges support from NIH New Innovator Award DP2 116520. P.N.K. also acknowledges the Edward R. Weidlein Chair Professorship funds for partial financial support of this research.

Disclosure Statement

No competing financial interests exist.

References

1. Daneman, D. Type 1 diabetes. Lancet **367,** 847, 2006.
2. Shapiro, A.M.J., Lakey, J.R.T., Ryan, E.A., Korbutt, G.S., Toth, E., Warnock, G.L., *et al.* Islet transplantation in seven patients with type 1 diabetes mellitus using a glucocorticoid-free immunosuppressive regimen. N Engl J Med **343,** 230, 2000.
3. Lanza, R.P., Borland, K.M., Staruk, J.E., Appel, M.C., Solomon, B.A., and Chick, W.L. Transplantation of encapsulated canine islets into spontaneously diabetic BB/Wor rats without immunosuppression. Endocrinology **131,** 637, 1992.
4. O'Shea, G.M., Goosen, M.F.A., and Sun, A.M. Prolonged survival of transplanted islets of Langerhans encapsulated in a biocompatible membrane. Biochim Biophys Acta (BBA) **804,** 133, 1984.
5. Maki, T., Otsu, I., O'Neil, J.J., Dunleavy, K., Mullon, C.J., Solomon, B.A., *et al.* Treatment of diabetes by xenogeneic islets without immunosuppression: use of a vascularized bioartificial pancreas. Diabetes **45,** 342, 1996.
6. Iwata, H., Amemiya, H., Matsuda, T., Takano, H., Hayashi, R., and Akutsu, T. Evaluation of microencapsulated islets in agarose-gel as bioartificial pancreas by studies of hormone-secretion in culture and by xenotransplantation. Diabetes **38,** 224, 1989.
7. Lee, K.Y., and Mooney, D.J. Alginate: properties and biomedical applications. Prog Polym Sci **37,** 106, 2012.
8. Leung, A., Nielsen, L.K., Trau, M., and Timmins, N.E. Tissue transplantation by stealth—coherent alginate microcapsules for immunoisolation. Biochem Eng J **48,** 337, 2010.
9. Shen, F., Mazumder, M.A., Burke, N.A., Stover, H.D., and Potter, M.A. Mechanically enhanced microcapsules for cellular gene therapy. J Biomed Mater Res B Appl Biomater **90,** 350, 2009.
10. Hillberg, A.L., Kathirgamanathan, K., Lam, J.B., Law, L.Y., Garkavenko, O., and Elliott, R.B. Improving alginate-poly-L-ornithine-alginate capsule biocompatibility through genipin crosslinking. J Biomed Mater Res B Appl Biomater **101,** 258, 2013.
11. O'Sullivan, E., Johnson, A., Omer, A., Hollister-Lock, J., Bonner-Weir, S., Colton, C., *et al.* Rat islet cell aggregates are superior to islets for transplantation in microcapsules. Diabetologia **53,** 937, 2010.
12. Lim, F., and Sun, A. Microencapsulated islets as bioartificial endocrine pancreas. Science **210,** 908, 1980.
13. Oshea, G.M., and Sun, A.M. Encapsulation of rat islets of langerhans prolongs xenograft survival in diabetic mice. Diabetes **35,** A82, 1986.
14. Duvivier-Kali, V.F., Omer, A., Parent, R.J., O'Neil, J.J., and Weir, G.C. Complete protection of islets against allorejection and autoimmunity by a simple barium-alginate membrane. Diabetes **50,** 1698, 2001.
15. Hoesli, C.A., Kiang, R.L.J., Mocinecová, D., Speck, M., Mošková, D.J., Donald-Hague, C., *et al.* Reversal of diabetes by βTC3 cells encapsulated in alginate beads generated by emulsion and internal gelation. J Biomed Mater Res B Appl Biomater **100B,** 1017, 2012.
16. Scharp, D.W., and Marchetti, P. Encapsulated islets for diabetes therapy: history, current progress, and critical issues requiring solution. Adv Drug Deliv Rev **67–68,** 35, 2014.
17. Steele, J.A.M., Hallé, J.P., Poncelet, D., and Neufeld, R.J. Therapeutic cell encapsulation techniques and applications in diabetes. Adv Drug Deliv Rev **67–68,** 74, 2014.
18. Dufrane, D., Goebbels, R.M., Saliez, A., Guiot, Y., and Gianello, P. Six-month survival of microencapsulated pig islets and alginate biocompatibility in primates: proof of concept. Transplantation **81,** 1345, 2006.
19. Tuch, B.E., Keogh, G.W., Williams, L.J., Wu, W., Foster, J.L., Vaithilingam, V., *et al.* Safety and viability of microencapsulated human islets transplanted into diabetic humans. Diabetes Care **32,** 1887, 2009.

20. Balamurugan, A.N., Bottino, R., Giannoukakis, N., and Smetanka, C. Prospective and challenges of islet transplantation for the therapy of autoimmune diabetes. Pancreas **32,** 231, 2006.
21. Segev, H., Fishman, B., Ziskind, A., Shulman, M., and Itskovitz-Eldor, J. Differentiation of human embryonic stem cells into insulin-producing clusters. Stem Cells **22,** 265, 2004.
22. Xu, X., Kahan, B., Forgianni, A., Jing, P., Jacobson, L., Browning, V., *et al.* Endoderm and pancreatic islet lineage differentiation from human embryonic stem cells. Cloning Stem Cells **8,** 96, 2006.
23. Baharvand, H., Jafary, H., Massumi, M., and Ashtiani, S.K. Generation of insulin-secreting cells from human embryonic stem cells. Dev Growth Differ **48,** 323, 2006.
24. D'Amour, K.A., Bang, A.G., Eliazer, S., Kelly, O.G., Agulnick, A.D., Smart, N.G., *et al.* Production of pancreatic hormone-expressing endocrine cells from human embryonic stem cells. Nat Biotechnol **24,** 1392, 2006.
25. Maguire, T., Novik, E., Schloss, R., and Yarmush, M. Alginate-PLL microencapsulation: Effect on the differentiation of embryonic stem cells into hepatocytes. Biotechnol Bioeng **93,** 581, 2006.
26. Li, L., Davidovich, A.E., Schloss, J.M., Chippada, U., Schloss, R.R., Langrana, N.A., *et al.* Neural lineage differentiation of embryonic stem cells within alginate microbeads. Biomaterials **32,** 4489, 2011.
27. Wang, N., Adams, G., Buttery, L., Falcone, F.H., and Stolnik, S. Alginate encapsulation technology supports embryonic stem cells differentiation into insulin-producing cells. J Biotechnol **144,** 304, 2009.
28. Siti-Ismail, N., Bishop, A.E., Polak, J.M., and Mantalaris, A. The benefit of human embryonic stem cell encapsulation for prolonged feeder-free maintenance. Biomaterials **29,** 3946, 2008.
29. Chayosumrit, M., Tuch, B., and Sidhu, K. Alginate microcapsule for propagation and directed differentiation of hESCs to definitive endoderm. Biomaterials **31,** 505, 2010.
30. Dean, S.K., Yulyana, Y., Williams, G., Sidhu, K.S., and Tuch, B.E. Differentiation of encapsulated embryonic stem cells after transplantation. Transplantation **82,** 1175, 2006.
31. Kim, J., Sachdev, P., and Sidhu, K. Alginate microcapsule as a 3D platform for the efficient differentiation of human embryonic stem cells to dopamine neurons. Stem Cell Res **11,** 978, 2013.
32. Jaramillo, M., and Banerjee, I. Endothelial cell co-culture mediates maturation of human embryonic stem cell to pancreatic insulin producing cells in a directed differentiation approach. J Vis Exp pii: 3759, 2012.
33. Watanabe, K., Ueno, M., Kamiya, D., Nishiyama, A., Matsumura, M., Wataya, T., *et al.* A ROCK inhibitor permits survival of dissociated human embryonic stem cells. Nat Biotechnol **25,** 681, 2007.
34. Heiligenstein, S., Cucchiarini, M., Laschke, M.W., Bohle, R.M., Kohn, D., Menger, M.D., *et al. In vitro* and *in vivo* characterization of nonbiomedical- and biomedical-grade alginates for articular chondrocyte transplantation. Tissue Eng Part C Methods **17,** 829, 2011.
35. Thomas, F.T., Contreras, J.L., Bilbao, G., Ricordi, C., Curiel, D., and Thomas, J.M. Anoikis, extracellular matrix, and apoptosis factors in isolated cell transplantation. Surgery **126,** 299, 1999.
36. Rezania, A., Bruin, J.E., Riedel, M.J., Mojibian, M., Asadi, A., Xu, J., *et al.* Maturation of human embryonic stem cell-derived pancreatic progenitors into functional islets capable of treating pre-existing diabetes in mice. Diabetes **61,** 2016, 2012.
37. Bruin, J.E., Rezania, A., Xu, J., Narayan, K., Fox, J.K., O'Neil, J.J., *et al.* Maturation and function of human embryonic stem cell-derived pancreatic progenitors in macroencapsulation devices following transplant into mice. Diabetologia **56,** 1987, 2013.
38. Cozar-Castellano, I., Fiaschi-Taesch, N., Bigatel, T.A., Takane, K.K., Garcia-Ocaña, A., Vasavada, R., *et al.* Molecular control of cell cycle progression in the pancreatic β-Cell. Endocr Rev **27,** 356, 2006.
39. Tuch, B.E., Hughes, T.C., and Evans, M.D. Encapsulated pancreatic progenitors derived from human embryonic stem cells as a therapy for insulin-dependent diabetes. Diabetes Metab Res Rev **27,** 928, 2011.
40. Martín, F., Andreu, E., Rovira, J.M., Pertusa, J.A., Raurell, M., Ripoll, C., *et al.* Mechanisms of glucose hypersensitivity in beta-cells from normoglycemic, partially pancreatectomized mice. Diabetes **48,** 1954, 1999.
41. Ungrin, M.D., Joshi, C., Nica, A., Bauwens, C., and Zandstra, P.W. Reproducible, ultra high-throughput formation of multicellular organization from single cell suspension-derived human embryonic stem cell aggregates. PLoS One **3,** e1565, 2008.
42. Nair, R., Ngangan, A.V., Kemp, M.L., and McDevitt, T.C. Gene expression signatures of extracellular matrix and growth factors during embryonic stem cell differentiation. PLoS One **7,** e42580, 2012.
43. Brafman, D.A., Phung, C., Kumar, N., and Willert, K. Regulation of endodermal differentiation of human embryonic stem cells through integrin-ECM interactions. Cell Death Differ **20,** 369, 2013.
44. Jones, L.E., Humphreys, M.J., Campbell, F., Neoptolemos, J.P., and Boyd, M.T. Comprehensive analysis of matrix metalloproteinase and tissue inhibitor expression in pancreatic cancer: increased expression of matrix metalloproteinase-7 predicts poor survival. Clin Cancer Res **10,** 2832, 2004.
45. Singh, A.M., Reynolds, D., Cliff, T., Ohtsuka, S., Mattheyses, A.L., Sun, Y.H., *et al.* Signaling network crosstalk in human pluripotent cells: a Smad2/3-regulated switch that controls the balance between self-renewal and differentiation. Cell Stem Cell **10,** 312, 2012.
46. Conery, A.R., Cao, Y.N., Thompson, E.A., Townsend, C.M., Ko, T.C., and Luo, K.X. Akt interacts directly with Smad3 to regulate the sensitivity to TGF-beta-induced apoptosis. Nat Cell Biol **6,** 366, 2004.
47. Remy, I., Montmarquette, A., and Michnick, S.W. PKB/Akt modulates TGF-beta signalling through a direct interaction with Smad3. Nat Cell Biol **6,** 358, 2004.

Address correspondence to:
Ipsita Banerjee, PhD
Department of Chemical Engineering
University of Pittsburgh
1242 Benedum Hall
3700 O'Hara Street
Pittsburgh, PA 15261

E-mail: ipb1@pitt.edu

Received: October 21, 2013
Accepted: May 28, 2014
Online Publication Date: July 15, 2014